Advances in Colloid and Interface Science 144 (2008) 54–65

Contents lists available at ScienceDirect

Advances in Colloid and Interface Science

journal homepage: www.elsevier.com/locate/cis

Kinetics of wetting and spreading by aqueous surfactant solutions

K.S. Lee [a], N. Ivanova [a], V.M. Starov [a,*], N. Hilal [b], V. Dutschk [c]

[a] Department of Chemical Engineering, Loughborough University, LE11 3TU, UK
[b] School of Chemical and Environmental Engineering, University of Nottingham, University Park, Nottingham, NG7 2RD, UK
[c] Leibniz Institute of Polymer Research Dresden, Germany

ARTICLE INFO

Available online 20 August 2008

Keywords:
Hydrophobic surfaces
Wetting kinetics
Spreading
Capillary imbibition
Superspreading

ABSTRACT

Interest in wetting dynamics processes has immensely increased during the past 10–15 years. In many industrial and medical applications, some strategies to control drop spreading on solid surfaces are being developed. One possibility is that a surfactant, a surface-active polymer, a polyelectrolyte or their mixture are added to a liquid (usually water). The main idea of the paper is to give an overview on some dynamic wetting and spreading phenomena in the presence of surfactants in the case of smooth or porous substrates, which can be either moderately or highly hydrophobic surfaces based on the literature data and the authors own investigations. Instability problems associated with spreading over dry or pre-wetted hydrophilic surfaces as well as over thin aqueous layers are briefly discussed. Toward a better understanding of the superspreading phenomenon, unusual wetting properties of trisiloxanes on hydrophobic surfaces are also discussed.

Contents

1. Introduction

Both wetting and de-wetting play an important role in many natural and technological processes. In many applications, surface wettability is macroscopically described by the equilibrium or, more frequently, by a static advancing contact angle. This description is mostly used to describe wetting properties of liquids on smooth, chemically homogeneous surfaces and pure liquids excluding adsorption and evaporation effects. However, such kind of approach is not sufficient for description of a host of technological processes as the kinetic aspects in the presence of surfactants should be considered. In a number of applications dynamic wetting and de-wetting processes are of crucial importance. The spreading velocity is often an important criterion based on which the efficiency of surface-active substances (surfactants) can be estimated.

The dynamic behaviour of a pure liquid on an ideal solid surface can often be successfully described by the equilibrium contact angle (or rather static advancing/receding contact angles), the dynamic (time-dependent) contact angle as well as the spreading velocity. Such approach [1,2] leads to the spreading force $\gamma_{lv}(\cos\theta_0 - \cos\theta(t))$, where θ_0 is the static advancing or receding contact angle. Note, in the case of spreading θ_0 should be selected as static advancing contact angle, while in the case of de-wetting θ_0 should be selected as static receding contact angle. Work is necessary to expanding the solid–liquid interface, and energy dissipates due to viscous shear in the liquid. The molecular-kinetic theory [3] assumes, however, particular displacements due to the surface diffusion at the three-phase contact line as a possible reason for the spreading force. It completely neglects viscous dissipation in the liquid and, hence, is suitable for describing of very slow velocities of spreading. Its application to predict the

* Corresponding author.
E-mail address: V.M.Starov@lboro.ac.uk (V.M. Starov).

0001-8686/$ – see front matter © 2008 Elsevier B.V. All rights reserved.
doi:10.1016/j.cis.2008.08.005

spreading velocity is rather problematic since the molecular parameters such as the density of the adsorption centres and the distance between them on real surfaces is unknown and generally inaccessible to experiments.

In general, when a liquid drop is placed on a solid surface, either it spreads over the surface, i.e. it completely wets it (Fig. 1a), or it forms a finite contact angle with the surface. If the contact angle is between 0 and 90° the situation is refereed to as partial wetting (Fig. 1b). However, if the contact angle is larger than 90°, the liquid does not wet the surface and the situation is refereed to as non-wetting (Fig. 1c). A more detailed description of advancing, receding, equilibrium and hysteresis contact angles as well as problems of experimental and theoretical verification of equilibrium contact angles have been recently provided [4,7].

A reduction of water surface tension by adsorption of surfactant molecules on a water-vapour interface and adsorption of surfactant molecules on solid–liquid and solid–vapour interfaces alters a non-wetting behaviour of aqueous solutions on hydrophobic substrates into a partial or even complete wetting behaviour. Surfactants have been used for a long time and their influence on surface wettability is well known and widely used. However, employing surfactants to enhance spreading complicates the wetting process through time-dependent diffusion and adsorption processes at the involved interfaces. The same processes are important in the case of water penetration into hydrophobic porous media. Aqueous surfactant solutions can spontaneously penetrate into hydrophobic porous substrates and the penetration rate depends on both the surfactant type and its concentration. Both the liquid–vapour interfacial tension γ_{lv} and the contact angle of moving meniscus, θ_a, (advancing contact angle) become concentration dependent.

The major process determining penetration of aqueous surfactant solutions into hydrophobic porous media or spreading over hydrophobic substrates seems to be the adsorption of surfactant molecules onto a bare hydrophobic substrate in front of the moving three-phase contact (TPC) line. The latter process results in a partial hydrophilisation of the hydrophobic surface in front of the meniscus or drop, which determines a spontaneous imbibition or spreading.

A pure water does not spontaneously penetrate into hydrophobic capillaries and shows the advancing contact angle larger than 90°. The latter means that water can be only forced into the capillary using an applied excess pressure or much easier by adding surface-active agents. Let us consider in more details a very beginning of the imbibition process into a hydrophobic capillary, when a surfactant solution touches the capillary inlet. The advancing contact angle at this moment is larger than 90° and the liquid can not penetrate into the capillary. Solid–liquid and liquid–vapour interfacial tensions do not vary with time on the initial stage, because the adsorption of surfactant molecules onto these surfaces is a relatively fast process compared with the imbibition rate. Only solid–vapour interfacial tension, γ_{sv}, can vary. If the adsorption of surfactant molecules at the bare hydrophobic surface in the vicinity of the TPC line takes place, the solid–vapour interfacial tension increases with time. After reaching some critical value, Γ_{sv}^{cr}, the advancing contact angle reaches 90° and the spontaneous imbibition process can start. The latter consideration shows that there is a critical bulk concentration, c_*, below which Γ_{sv} remains below it's critical value Γ_{sv}^{cr} and the spontaneous imbibition process does not take place.

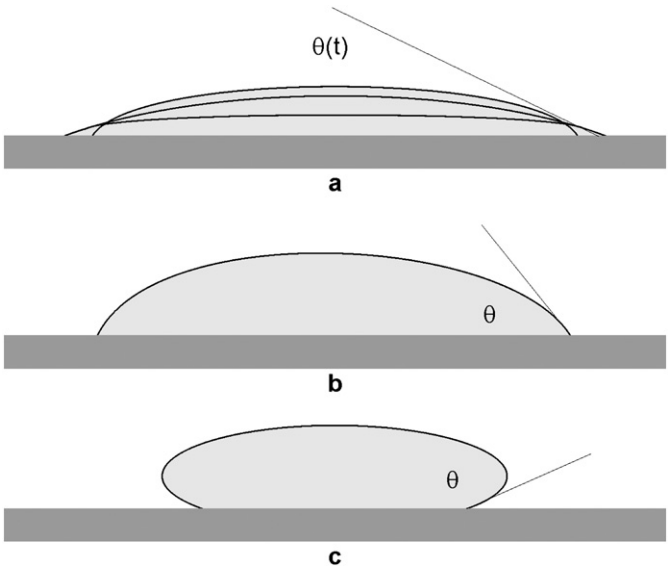

Fig. 1. Different wetting situations: (a) complete wetting case: a droplet completely spreads out and only dynamic contact angle can be measured, which tends to zero over time; (b) partial wetting case: the contact angle is in between 0 and 90°; non-wetting case: the contact angle is larger than 90°.

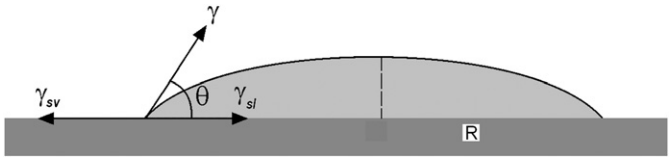

Fig. 2. Schematic of a droplet placed on a solid surface; γ, γ_{sl} and γ_{sv} are liquid–vapour, solid–liquid and solid–vapour interfacial tension, respectively, at the three-phase contact line; R is the radius of the droplet base. The droplet is small enough and the gravity action can be neglected.

The excess free energy Φ of the droplet deposited on a solid substrate Fig. 2 is as follows:

$$\Phi=\gamma S+PV+\pi R^2(\gamma_{sl}-\gamma_{sv}), \quad (1)$$

where S is the area of the liquid–vapour interface; $P=P_a-P_l$ is the excess pressure inside the liquid, P_a and P_l are the ambient air pressure and pressure inside the liquid, respectively; R is droplet base radius; γ, γ_{sl} and γ_{sv} are the liquid–vapour, solid–liquid and solid vapour interfacial tensions, respectively. The last term in the right hand site of Eq. (1) gives the difference between the energy of the surface covered by the liquid drop and the energy of the same solid surface without the droplet. Eq. (1) shows that the excess free energy decreases if (a) the liquid–vapour interfacial tension decreases; (b) the solid–liquid interfacial tension decreases; and (c) the solid–vapour interfacial tension increases. The latter very important conclusion is often overlooked.

In the absence of surfactants, the drop forms a contact angle above 90° with a hydrophobic substrate. In the presence of surfactants the following three transfer processes take place from the liquid onto all three interfaces: surfactant adsorption at both (i) the inner solid–liquid interface and (ii) the liquid–vapour interface, and (iii) transfer of surfactant molecules from the drop onto the solid–vapour interface in front of the drop on the bare hydrophobic substrate. As mentioned above, all three processes lead to a decrease of the excess free energy of the system. However, adsorption processes (i) and (ii) result in a decrease of corresponding interfacial tensions γ_{sl} and γ, but the transfer of surfactant molecules onto the solid–vapour interface in front of the drop results in an increase of a local free energy, however, the total free energy of the system decreases according to Eq. (1). That is, surfactant molecule transfer (iii) goes via a relatively high potential barrier and, hence, goes considerably slower than adsorption processes (i) and (ii). Hence, processes (i) and (ii) are "fast" processes compared with the "slow" third process (iii).

Despite the enormous technical importance of spreading of aqueous surfactant solutions over solid surfaces, information on possible spreading mechanisms is still limited in the literature. Disjoining

pressure isotherms in the presence of surfactants are well investigated in the case of free liquid films [5], much less is known in the case of liquid films on solid substrates [6]. At the present, we are not able to provide a clear definite mechanism of surfactant molecules transfer on a bare hydrophobic substrate in front of in a vicinity of the moving TPC line. The reason is that in the case of aqueous surfactant solutions our knowledge of the transition zone between meniscus/droplet to thin films in front is still very limited.

It was shown in [7] that the well known Young's equation for the equilibrium contact angle as an empirical one and should be replaced by Derjaguin–Frumkin equation. The latter equation expresses the equilibrium contact angle via measurable physical properties, which are surface forces acting in the TPC line vicinity. However, in view of our limited knowledge regarding the surfactant behaviour in the vicinity of moving TPC line we use below Young's equation for describing spreading processes over hydrophobic surfaces. Our hypothesis on surfactants adsorption at a bare hydrophobic substrate in front of the moving meniscus/droplet allows us to develop some theoretical predictions, which are in a reasonable agreement with known experimental data in the literature.

The situation is even less investigated in the case of simultaneous spreading and imbibition into porous substrate. We present some theoretical and experimental investigations of the process, which should be considered as a first step in this direction.

We also consider much better theoretically understood process of flow caused by the surface tension gradient (Marangoni flow). It was shown earlier that the flow caused by the surfactant point source on the surface of a thin aqueous film is governed by the surface tension gradient only. This process recently became a powerful tool for investigation the phenomenon of superspreading.

2. Spreading over hydrophobic substrates

In the following the results published in the area over the last two decades are summarised.

Keurentjes et al. [8] investigated the effect of surface hydrophobicity on surfactant adsorption onto the interfaces. Surfactant adsorbed onto the hydrophobic surface exposes its polar head groups to the solution, whereas in the case of a more polar surface, surfactant molecules bilayers may form rendering the surface more hydrophilic. These adsorption phenomena can be explained in a semi-quantitative way by taking the cooperative nature of surfactant adsorption into account and making estimates of free energies for various conceivable interfaces in the system.

Scales et al. [9] shown that the contact angle and adsorption density data may be combined to provide useful information to the adsorption mode at solid surfaces of a series of alkyl–aryl–polyoxyethylenes.

von Bahr et al. [10] observed that wetting at low surfactant concentrations proceeds in two stages — a short time regime where spreading occurs rapidly, and a long time regime where spreading is slow. According to [10], the rate-limiting process in the drop spreading experiment was assumed to be the surfactant adsorption from the bulk to the expanding liquid–vapour interface. During the initial spreading phase, surfactant molecules adsorb at the expanding solid–liquid interface behind the moving liquid, as shown in Fig. 3.

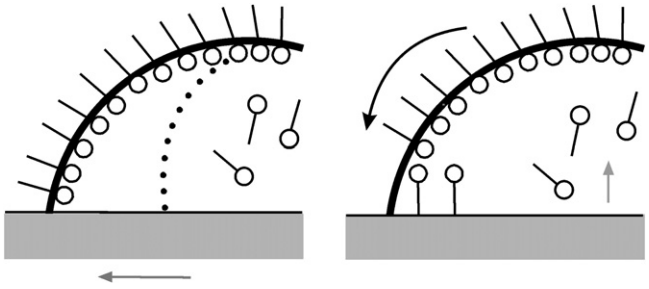

Fig. 3. Spreading mechanism of aqueous surfactant solutions on hydrophobic surfaces according to von Bahr et al. [10]. During the initial spreading phase, surfactant molecules adsorb at the expanding solid–liquid interface behind the moving liquid. Simplistically, we abstain here from the illustration of adsorbed surfactant layer at the solid–liquid interface. From [16].

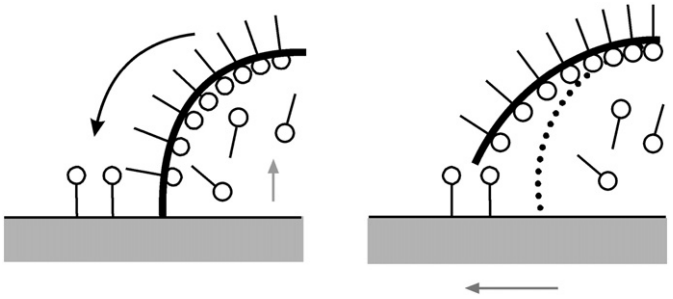

Fig. 4. Spreading mechanism of aqueous surfactants solutions on hydrophobic surfaces according to Starov et al. [12]. From [16].

Dutschk et al. [11] observed the wetting behaviour of dilute ionic and non-ionic aqueous surfactant solutions over highly and moderately hydrophobic polymer surfaces. They found that non-ionic surfactants enhanced spreading over both type of surfaces, whereas ionic surfactants do not spread over highly hydrophobic surfaces. They took evaporation factor into account and presented a theory to correct the contact angle measured. Two spreading regimes observed: a short time (fast spreading) regime and long time (slow spreading) one. They argued in their case, the long time regime goes much slower than predicted in [10], and concluded there exists a possible explanation where adsorption at the expanding solid–liquid interface goes more slowly than diffusion.

Starov et al. [12] described the spreading mechanism of aqueous surfactant solutions over hydrophobic surfaces as a slow transfer of surfactant molecules on the bare hydrophobic surfaces in front of the moving liquid on the TPC line (Fig. 4). This mechanism was suggested earlier in [13–15]. In [12] the authors predicted the dynamic droplet radius and contact angle for a system where surfactant solutions spread over hydrophobic substrates. In the theoretical treatment an assumption was made that the transfer of surfactant molecules onto bare hydrophobic substrate in front is the rate determining step. According to the model suggested in [12] the contact angle changes as follows

$$\cos\theta(t) = \cos\theta_0 + (\cos\theta_\infty - \cos\theta_0)(1 - \exp(-t/\tau)), \quad (2)$$

where θ_0 and θ_∞ are the initial and final contact angles, respectively; τ is a time scale of surfactant molecules transfer on a bare hydrophobic

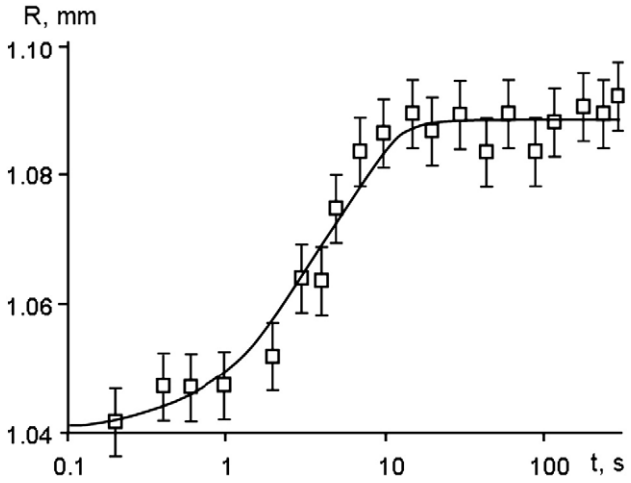

Fig. 5. Base radius of a water drop (aqueous SDS solution $c = 0.05\%$, 2.5 ± 0.2 μl volume) as a function of time on PTFE. Error bars correspond to the error limits of video evaluation of images (pixel size). From [12].

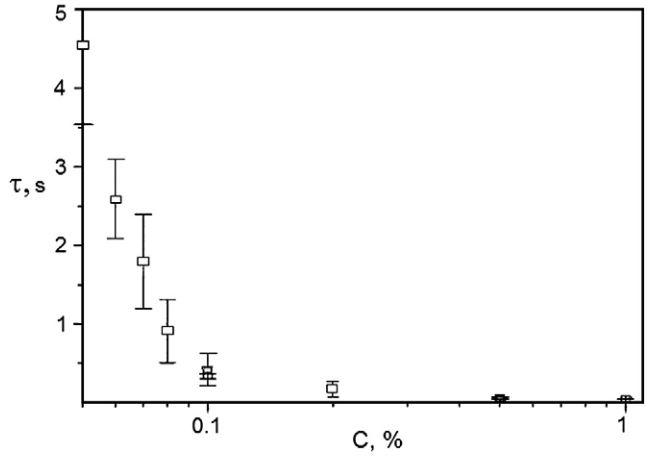

Fig. 6. Fitted dependency of τ on SDS surfactant concentration inside the drop (spreading over PTFE). Error bars correspond to the experimental points scattering in different runs; squares are average values. From [12].

substrate in front of the moving TPC line. The latter equation coupled with the conservation of the drop volume results in an equation for the radius of the drop base [12].

The theoretical prediction corresponds well to the experimental data (Fig. 5), and a justification was presented for the assumption concerning the transfer mechanism of surfactant molecules (Fig. 6). It was assumed that transfer of surfactant molecules onto the hydrophobic solid interface takes place only from the liquid–vapour interface as shown in Fig. 4. Experimental data presented in Fig. 6 support this assumption, although they do not prove it decisively. The surface coverage of the liquid–vapour interface of the drop is an increasing function of the bulk surfactant concentration inside the drop. The maximum surface coverage is reached close to the critical micelle concentration (CMC). Hence, according to this mechanism at low surfactant concentrations inside the drop, the characteristic time scale of the surfactant molecules transfer, τ, decreases with increased concentration, while above the CMC τ should level off and reach its lowest value. Both of these effects are experimentally confirmed in [12] (see Fig. 6).

The presence of surfactant molecules increases the solid–vapour interfacial tension and hydrophilize the initially hydrophobic solid substrate in front of the spreading drop. This process causes the spreading. The absence of adsorbed water molecules in front of the drop plays its part in making the spreading a very slow process. The analysis of time dependencies of the drop base radius [16] reveals that the slow wetting dynamics observed for both ionic and non-ionic surfactants on hydrophobic surfaces can be explained neither by surfactant diffusion from the bulk of the drop to the expanding liquid–vapour interface nor in terms of viscous spreading. Two possible mechanisms were suggested [16]: (a) a slow rearrangement of surfactant molecules adsorbed at the solid–liquid interface, which occurs inside the drop, possible caused by the bi-layer formation due to low monomer solubility which, in turn, may be affected by low surrounding humidity leading to water evaporation from the drop; (b) the transfer of surfactant molecules onto the bare hydrophobic surfaces which is a relatively slow but a spontaneous process [12]. The characteristic time scale of the surfactant molecules transfer onto the hydrophobic surface decreases with increasing surfactant concentration for all surfactant/polymer systems studied as predicted in [12]. Experimental data in [11,16,17] indicate that the latter mechanism is valid for both highly and moderately hydrophobic surfaces. Moreover, it was found that the characteristic time scale for transfer of individual ethoxylated alcohol surfactants C_mEO_5 estimated for hydrophobic polypropylene surface increases with increasing the hydrocarbon chain length, probably indicating steric limitations with increasing molecular size. As concluded in [16], based on experimental data the characteristic time scale τ of surfactant molecules transfer, which can be considered as a spreading characteristic, sensibly responds to changes of both the surfactant nature (ionic, non-ionic) and surface free energy.

Eriksson et al. [18] monitored the interfacial adsorption and interfacial tension to further understand how wetting is influenced by surfactant transfer to the TPC line and provided further support to claims that surfactant transfer to the TPC line is dominant. Frank et al. [19] observed that changes in the spreading behaviour are due to the adsorption of a surfactant ahead of the contact line.

Chan et al. [20] developed a mathematical model for surfactant enhanced spreading. They suggested two additional mechanisms that influence the spreading rate: the development of positive surface curvature near the moving contact line, which produces a favourable radial pressure gradient within the drop, and the surfactant convection in a vicinity of the moving contact line.

3. Spontaneous rise and imbibition of surfactant solutions into hydrophobic capillaries

In the case of the partial wetting when an advanced contact angle takes on values $0<\theta_a<\pi/2$ the penetration of a liquid into a horizontal or vertical (at short times) capillary is described by the following equation [21]:

$$z(t)=\left(\frac{R\gamma\cos\theta_a}{2\eta}t\right)^{1/2}, \tag{3}$$

where the subscript a indicates the advancing contact angle, $z(t)$ is the length of part of the capillary filled with the liquid, R is the capillary radius, γ is the liquid–vapour interfacial tension, η is the dynamic liquid viscosity, t is time.

In the case of a vertical capillary, the law of liquid penetration corresponding to the long time limit, when a liquid rises to a stationary level $z_\infty=2\gamma\cos\theta_a/\rho gR$ where gravity balances the capillary force, is given by equation [22]

$$z(t)=z_\infty\left[1-\exp\left(-\frac{\rho gR^2}{8\eta z_\infty}t\right)\right], \tag{4}$$

where ρ is the liquid density and g is the gravity acceleration.

When the advancing contact angle $\theta_a>\pi/2$, pure water does not penetrate spontaneously into the hydrophobic capillaries. In this case the liquids can be forced into the capillaries by applying external fields such as a pressure force, electrowetting [23] or thermocapillary forces [24].

However, as it was found in [13–15,25] aqueous surfactant solutions penetrate spontaneously into hydrophobic capillaries. It was shown that adsorption of the surfactant molecules onto the capillary walls ahead of a moving meniscus makes possible the penetration of surfactant solutions into the hydrophobic capillaries. It is assumed that surfactant molecules adsorption onto the solid–liquid and liquid–vapour interfaces proceeds much faster compared with the characteristic time scale of penetration. The latter means that the interfacial tensions γ_{sl} and γ near meniscus do not change considerably over time because adsorption processes are sufficiently fast. Indeed, the experiments on the spontaneous capillary imbibition of Syntamide-5 aqueous solutions into horizontal hydrophobic capillaries [13,15] (Fig. 7) have shown that characteristic time scales of the imbibition and rise are being around 100 s and 10^5 s, respectively, while a time scale estimation of diffusion kinetics in the capillary cross-section is only around $R^2/D\approx0.1$ s ($R\sim10$ μm and $D\sim10^{-5}$ cm^2/s) [25,26].

Adsorption of surfactant molecules on the solid–vapour interface leads to an increase of its interfacial tension with time and

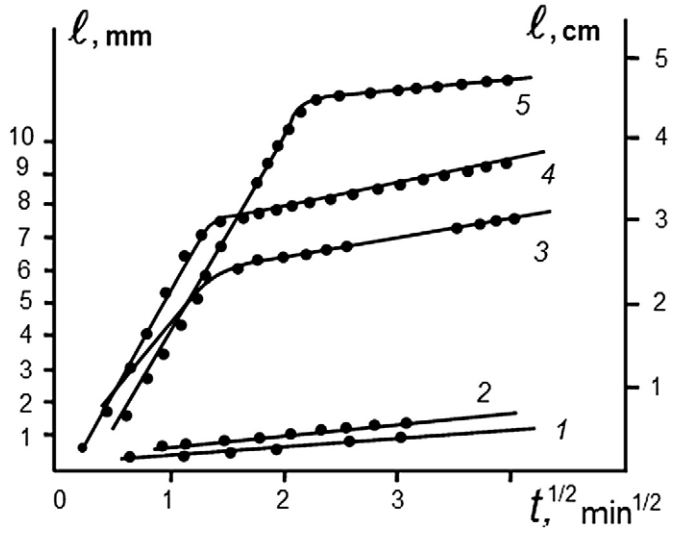

Fig. 7. Time evolution of the imbibition length l (mm) with time, t (min) for aqueous solutions of Syntamide-5 in a horizontal hydrophobized quartz capillary with $R=16$ μm: (1) $c_0=0.05\%$; (2) $c_0=0.1\%$; (3) $c_0=0.4\%$; (4) $c_0=0.5\%$; (5) $c_0=1\%$. From [15,7].

consequently to a decrease of the advancing contact angle, which becomes $\theta_a<\pi/2$ at some critical adsorption of surfactants corresponding to a critical bulk concentration, c_* [13–15,25]. The spontaneous imbibition into the hydrophobic capillary commences when the concentration of surfactant in solution c_0 is above c_*, that is at $c_0>c_*$. A theoretical analysis of a spontaneous imbibition of surfactant solutions into hydrophobic capillaries, taking into account the convective transfer, the surface diffusion of surfactant molecules and the adsorption of molecules on a hydrophobic surface was reported in [14–15,26].

The mechanisms of spontaneous imbibition is assumed to be controlled by surfactant concentration c_m close to the moving meniscus, which is below c_0. Hence, the expression $\gamma\cos\theta_a$ in Eq. (3) should depend on the concentration c_m. It was shown in [13–15,25,26] that the dependency $\varphi(c_m)=\gamma\cos\theta_a$ can be approximated as

$$\varphi(c_m)=\alpha(c_m-c_*), \tag{5}$$

where the coefficient α was calculated in [25]. According to Eq. (5), $\varphi(c_m)$ should be a linear function of concentration at $c_m>c_*$, which is in agreement with experimental results [14,15]. In the case of the surfactant concentration c_0 is below the CMC, the imbibition rate according to Eqs. (3) and (5) can be represented as follows [25,26]

$$z(t)=\left(\frac{R\alpha(c_m-c_*)}{2\mu}t\right)^{1/2}. \tag{6}$$

The surfactant concentration c_m near the moving meniscus remains constant in time ($c_m=$const) and its value depends on the diffusion coefficient and adsorption characteristics of surfactant molecules.

If the surfactant concentration c_0 is above the CMC, the adsorption of surfactant molecules on the solid–vapour interface in front of the moving meniscus leads to a disintegration of micelles decreasing the surfactant concentration c_m from $c_m=c_0>$CMC to $c_m<$CMC. At the moment when the $c_m=$CMC the imbibition rate abruptly changed, which was caused by a separation of the micelle front from meniscus. The latter resulted in a corresponding decreasing of c_m and as a consequence in a slower kinetics of imbibition into the hydrophobic capillary. After that moment the concentration c_m no longer changed and remained below the CMC; the second slower stage of the process started. The micelle front moves according to the same power law as in Eq. (3), but rather slower then the meniscus. As appears from the above analysis, the imbibition process at concentrations $c_0>$CMC should be characterized by two stages. Indeed, the experiments on the penetration of aqueous solutions of Syntamide-5 [13,15] into the hydrophobic capillaries clearly shown an existence of the two kinetic stages. The second stage is substantially slower than the first stage because only individual surfactant molecules move with the meniscus. Note, during the slower second stage, the spontaneous imbibition rate is only slightly higher than that in the case when the concentration of surfactant c_0 is below the CMC.

Unlike the case of the spontaneous imbibition of surfactant solutions into a flat hydrophobic capillary, where the concentration of surfactant c_m near the meniscus is constant, the spontaneous rise into a vertical hydrophobic capillary is controlled by a different mechanism, because the concentration c_m can not remain constant. Spontaneous capillary rise experiments with Syntamide-5 solutions in a vertical hydrophobized quartz capillary [13] showed that the time evolution of the rise satisfies Eq. (3) at the initial stage of the process. However, the slopes dependencies $z(\sqrt{t})$corresponds to the θ_a values being only a few seconds less than $\pi/2$. At such θ_a values, the capillary rise would be expected to stop when the liquid reached a level of $z_{max}\sim 10^{-3}$ cm. However, it does not stop at this level and goes up to a height of 3–4 cm. The explanation of this effect is that the meniscus rises following the surface diffusion front of surfactant molecules, which hydrophilise the walls of capillary in front of the moving meniscus [15,25]. It was shown that the position of the solution meniscus should be described by equation

$$z(t)=\frac{2\alpha}{\rho g h}(c_m-c_*), \tag{7}$$

which is valid only if $c_m(t)$ increases with time and, hence, the concentration of surfactant $c_m(t)$ near the meniscus in the case of spontaneous capillary rise into a hydrophobic capillary does not remain constant. The maximum level of the capillary rise z_{max} is reached after the concentration c_m becomes equal to the concentration at the capillary inlet c_0. Then, the rise stops at the maximum height determined as follows

$$z_{max}=\frac{2\alpha}{\rho g h}(c_0-c_*). \tag{8}$$

The latter means that the experimental data presented in [15] correspond mostly to the initial stage of the capillary rise, $z(t)\ll z_{max}$, as shown in Fig. 8. The latter figure shows that the experimental data deviate from the straight line in accordance with theoretical considerations presented in [25]. These theoretical considerations were also confirmed in [27] where the spontaneous rise of $C_{10}E_6$ and

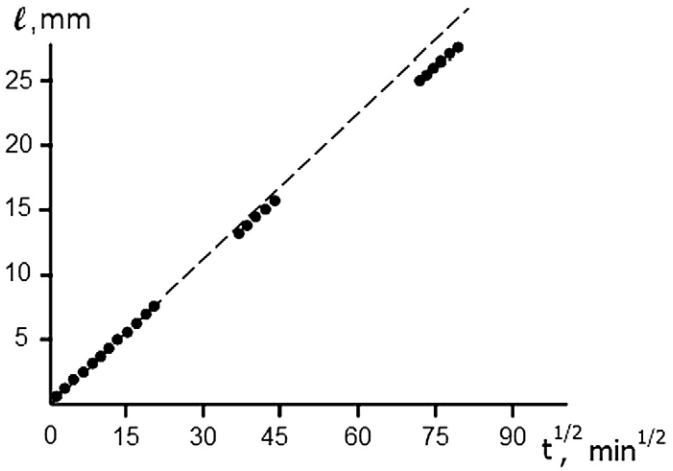

Fig. 8. Spontaneous capillary rise in a vertical hydrophobised quartz capillary ($R=11$ μm), Syntamid-5 surfactant solution ($c_0=0.1\%$). Time evolution of the imbibition length. From [7].

$C_{14}E_6$ aqueous solutions into hydrophobic cylindrical capillaries was reported. During the initial stage of the process position of the moving meniscus, $z(t)$, described by $z(t)\sim\sqrt{t}$ as in [25]. At the final stage, the meniscus moves towards the equilibrium level as predicted in [25]. It was also observed in [27] that for the same concentration $C_{10}E_6$ solutions rise faster than $C_{14}E_6$ solutions. The velocity of the capillary rise was also considered in [28].

4. Capillary imbibition into partially wetted porous medium

Starov et al. [29] investigated the capillary imbibition of surfactant solutions into dry porous substrates in the case of partial wetting. The cylindrical capillaries were used as a model of porous media to study the problem theoretically. Nitrocellulose membranes partially wetted by water were used to study the same process experimentally. For all concentrations, it was shown that the penetration rate obeys to Lucas–Washburn law. However, it was found that there is a critical capillary radius determined by adsorption of surfactant molecules onto the inner capillary surface

$$R_{cr}>R\frac{c_0^2}{CMC^2} \tag{9}$$

where $R_{cr}=\frac{\Gamma_\infty^2\pi\varphi_{max}}{2D\eta CMC^2}$, D is the diffusion coefficient of surfactant, η is the liquid viscosity, Γ_∞ is the maximum surface coverage, $\varphi_{max}=\gamma(CMC)\cos\theta_a(CMC)$.

If $R<R_{cr}$, then the permeability of porous medium is not influenced by the presence of surfactants in the feed solution, whatever the value of the concentration is. In this case all surfactant molecules are adsorbed on the capillary wall and nothing is left for the advancing meniscus. Note, the adsorption strength in a porous medium is proportional to the surface per unit volume, which is inversely proportional to the capillary radius in the case of a cylindrical capillary. On the other hand, the imbibition rate is lower in thinner capillaries due to higher friction. This gives more time for diffusion to bring new surfactant molecules to cover the fresh part of capillary walls. However, if the capillary radius is below the critical value, $R<R_{cr}$, then adsorption proceeds faster than imbibition and consumes all surfactant molecules from the solution. Thus, for thin capillaries (or fine porous media) the imbibition rate of surfactant solutions is independent of the surfactant concentration in the feed solution and takes a value equal to that in the case of pure water.

When the mean pore size is larger than the critical value, that is $R>R_{cr}$, then the permeability increases with increasing surfactant concentration. The theoretical conclusions are in agreement with experimental results presented in Fig. 9, where k is the permeability of porous membranes, and p_c is an effective capillary pressure inside the porous membrane.

Hodgson and Berg [30] studied imbibition of various pure liquids and surfactant solutions over wide range in concentrations in partially wetted strips of paper cut from cellulose filters. For all liquids, it was shown, that the penetration rate obeys to Lucas–Washburn law. It was found that the penetration rate in the case of partial wetting depends on the adhesion tension, which is represented as a difference $\gamma_{sv}-\gamma_{sl}$. Differences in imbibition of surfactant solutions was explained by differences in their adsorption and diffusive abilities.

5. Spreading of surfactant solutions over thin aqueous layers: influence of solubility and micelles disintegration

Thin liquid films can be found in many engineering, geology, and biophysics environment. Their applications are significant in many coating processes [31–32] and physiological applications [33]. Presence of non-uniform temperature or surface-active compounds along the surface of thin liquid films leads to formation of shear stresses, also known as Marangoni gradients at the liquid–vapour

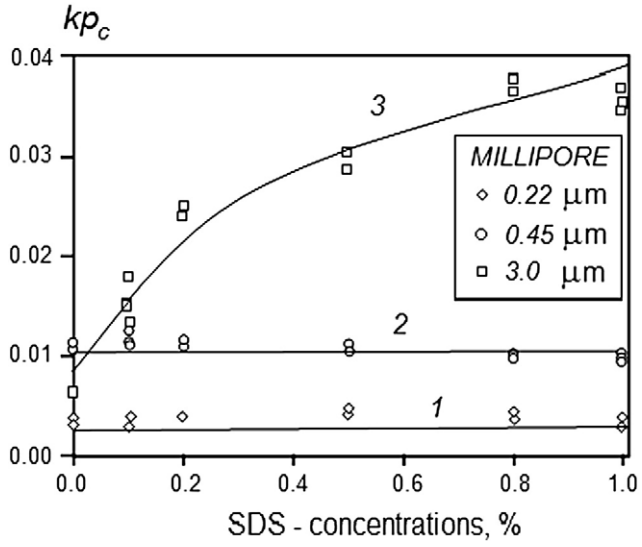

Fig. 9. Experimental values of kp_c versus concentration of a SDS solution for nitrocellulose membranes with different mean pore sizes (inset). kp_c remains constant in the case of membranes with both 0.22 μm (straight line 1) and 0.45 μm (straight line 2) mean pore size, while it increases with the increase in surfactant concentration for the membrane with mean pore size 3 μm (line 3). From [29].

interface. These gradients cause mass transfer on and in the liquid layer due to surface tension non-uniformity. Marangoni stresses distribute the liquid from areas of low surface tension to areas of high surface tension (flow generation) and in doing so also deform the interface resulting in variations of the film thickness (deformation and even possible instability of liquid films). In this section, we restrict our discussion of the influence of surfactants on thin liquid films.

An understanding of Marangoni induced flows is important as it can be beneficial or detrimental in many applications. Surfactants are normally present in a healthy mammalian lung to reduce surface tension forces. Surfactants keep the lungs compliant and prevent collapse of the small airways during exhalation. However, most prematurely born babies do not produce adequate amount of those surfactants. The latter leads to respiratory distress syndrome. This condition is treated by surfactant replacement therapy where surfactants are introduced into the lungs. These surfactants spread in the large to medium pulmonary airways. In small airways surface tension gradients dominate and Marangoni flow distributes the surfactant to the distal regions of the lung [34,35].

In coating processes paint films are dried by solvent evaporation. The non-uniformity of the evaporation leads to Marangoni stresses which cause deformation of the film and, hence, formation of defects on the paint surface [36]. Another example is a drying of films of latex suspensions (stabilised by surfactants). The drying process results in the surfactant non-uniformities (surfactant islands) that leave permanent indentations in the film [37].

The Marangoni effect is used for drying silicon wafers after a wet processing step during the manufacturing of integrated circuits. An alcohol vapour is blown through a moving nozzle over the wet wafer surface and the subsequent Marangoni effect causes the liquid on the wafer to pull itself off the surface effectively leaving a dry wafer surface [38].

Spreading of surfactant solutions on thin liquid films was reviewed by Afsar-Siddiqui et al. [39] a few years ago. It is the reason why below we summarize the progress made over the recent years only.

A moving circular wave front forms after a small droplet of aqueous surfactant solution is deposited on a thin aqueous layer as illustrated in Fig. 10. It was shown earlier [41] that this process has a very remarkable feature: all forces but Marangoni forces can be safely neglected.

The time evolution of the moving front radius was monitored [40], where an experimental methodology was designed to investigate the influence of Marangoni force on spreading of surfactant solutions over

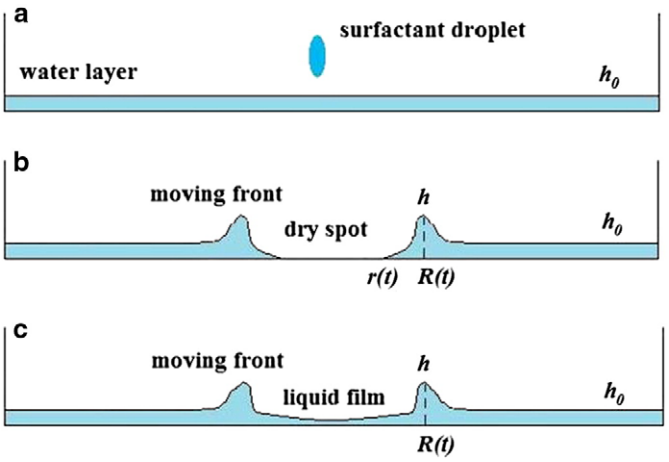

Fig. 10. (a) A small droplet of aqueous surfactant solution is deposited on a top of thin aqueous layer of thickness h_0; (b) dry spot formation in the centre: cross-section of the system: $R(t)$ is radius of a circular moving front, $r(t)$ is radius of dry spot in the centre, h is the height of the moving front; (c) the same as in the previous case (b) without dry spot formation in the centre. From [40].

thin aqueous layers. Surfactants with different solubility at concentrations above the CMC were used. In all cases [40] two stages of the front motion were observed: the first fast stage, which followed by a slower second stage. Both the first and the second stages of spreading considerably depend on the solubility of surfactants: the higher solubility the slower both stages. If the solubility is high enough then during the second stage the front reaches some final position and does not move any further. The lower solubility the higher the exponent in the spreading law $R(t)=\text{const}\cdot t^n$ during the first stage and for low soluble surfactants it reaches $n=0.75$. Moreover, it was shown that formation of a dry spot in the centre is determined by the speed of the first stage: the higher this speed the lower probability to have a dry spot formation. Hence, the dry spot forms in the case of soluble surfactants and does not form in the case of insoluble surfactants.

The observations in [40] differed from the earlier theoretical approach [41], thus the influence of surfactants solubility and disintegration of micelles were incorporated to improve on the previous theoretical model. According to the theoretical predictions in [40], low soluble surfactant produced both faster 1st and 2nd stage. Low soluble surfactant (Tween® 20) produced during the first stage a power law exponent 0.73 ± 0.01, being closest to the maximum attainable spreading rate 0.75 predicted theoretically [40]. For highly soluble surfactant DTAB, the solubility was most significant during the second stage, where the spreading front reached some final position and does not move any further in the agreement with the theoretical predictions [40].

6. Instabilities in the course of spreading

Instability at the contact line of surfactant solutions drops, spreading on dry or pre-wetted hydrophilic surfaces, leads to the fingering patterns formation at the edge of drops. Fingering at the contact line of drops of surfactant solutions spreading on solid substrates was firstly observed by Marmur et al. [42]. After that it was studied theoretically, experimentally as well as using numerical simulations [39,43–63]. It was assumed, that a water film pre-existing on the substrate was essential for the growth of the instability. In [43,54,55] investigations of spreading of non-ionic surfactants solutions in ethylene glycol or diethylene glycol on oxidised silicon wafers were carried out. The use of polar solvents different from water allowed the authors to discriminate between the role of a pre-existing adsorbed water film, which is known to be always present on a hydrophilic substrate in contact with the atmosphere, and the role of a possibly thicker film built up by the same liquid as the drop.

Troian et al. [50] proposed that the Marangoni effect is responsible for the instability at the edge of the spreading surfactant drop. The Marangoni flow at the interface and the bulk liquid is induced by gradients of surfactant concentration along the air–water interface. In their experiments [50], a 2 μl drop of aqueous AOT (sodium bis-(2-ethyl-hexyl) sulfosuccinate) solution placed on a hydrophilic surface covered with a thin water film, spreads by immediately forming fingers advancing from the contact line. The authors found that the drops of aqueous AOT solutions with concentration below the CMC (0.03 mM) and higher the CMC (10 mM) spread by uniform circularly edge. Surface tension difference between the AOT solution and pure water at low surfactant concentrations is not high enough and the surface tension gradient is insufficient to initiate the instability. Transport of excess surfactant from the bulk to the surface of the spreading drop at high AOT concentrations may suppress the formation of surface tension gradients and Marangoni flow. The maximum spreading rate of a 1 mM AOT solution drop reached up to 1 cm/s. It was found that the velocity and shape of fingers at intermediate AOT concentrations depend on the thickness of the underlying film and the surfactant concentration. On a thin (0.1 μm) water film fingers are narrow, sharply tipped and more branched, than those on a thick (1 μm) film, as shown in Fig. 11. The length of fingers during spreading depends on time as t^{α}, where $\alpha=0.66$ and 0.7 for the thin and thick films, correspondingly.

Frank and Garoff [51] determined that the formation of fingering patterns depends not only on the surfactant concentration gradients, but on a mechanism of surfactants-surface interactions. The same surfactant can exhibit fingering or stick-jump spreading behaviour on the same charged or opposite charged substrates, correspondingly. The spreading behaviour of aqueous anionic SDS (sodium dodecyl sulphate) and cationic CTAB (cetyltrimethylammonium bromide) surfactant solutions on a clean and dry oxidized silicone wafer and a polished sapphire disk were examined. The SDS solution spreads with the fingering formation on the silicone wafer, while on the sapphire substrate it exhibits an autophobing spreading. The spreading behaviour of CTAB solution on these substrates is just opposite to the behaviour of SDS solutions. Moreover, the authors [51] have shown also that on substrates, which had been pre-wetted with a surfactant solution monolayer, the fingering spreading was not observed. Furthermore, using the optical reflectivity measurements a precursor film ahead of the spreading front was detected on the

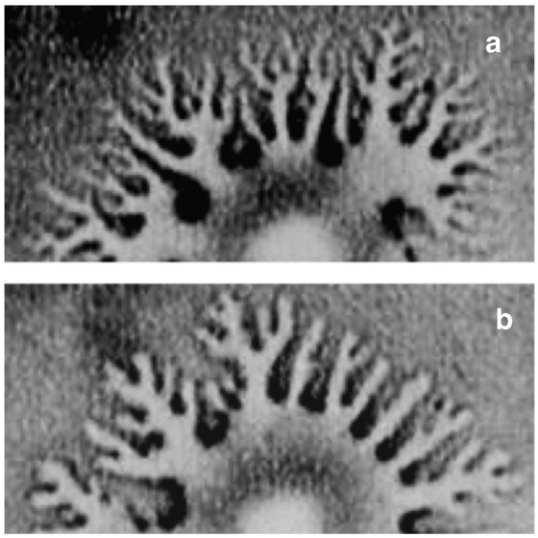

Fig. 11. Photographs of spreading drop at 0.5 s after its deposition; (a) fingering on a thin water layer; (b) fingering on a thick water layer [50].

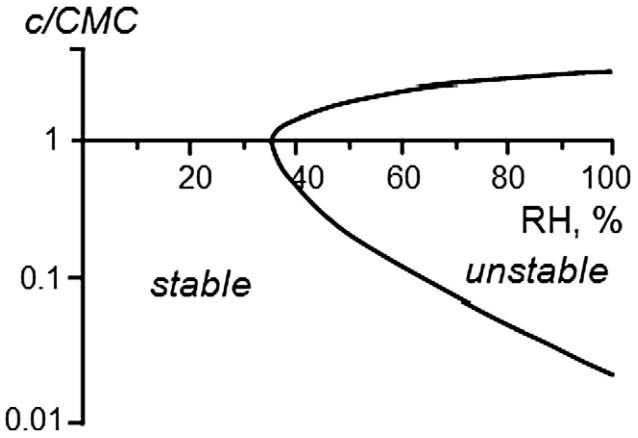

Fig. 12. "Phase diagram" of the behaviour of $C_{12}E_{10}$ in ethylene glycol as a function of the surfactant concentration relative to the CMC and RH [54].

initially dry substrates. Thus, the thin film exists on the surface that were not coated with water initially, and this film serves for mobilization surfactants and generation of the surfactant concentration gradient.

The role of the precursor films on the substrates and viscosity of solvents on the formation of the hydrodynamic instabilities at the contact line of the spreading drops has been intensively investigated by Cazabat and co-workers [43,54,55,56,57]. Cachile and Cazabat [54,55] studied the influence of ambient relative humidity (RH) and the surfactant concentration on the fingering spreading of aqueous non-ionic $C_{12}E_4$ and $C_{12}E_{10}$ surfactant solutions in ethylene and diethylene glycol on hydrophilic silicon wafers. Substrates used were oxidized silicon wafers cleaned with ultraviolet illumination in the presence of an oxygen flow. The experiments were carrying out in a humidity controlled cell. Ellipsometric measurements showed that the thickness of the adsorbed water film on silicone wafers does not exceed 5 Å at the high humidity RH=85%. The results were summarized in "phase diagram" as a function of the normalized surfactant concentration defined as the ratio of the bulk concentration to the CMC, and the relative humidity, RH (Fig. 12).

In the stable region, at the RH≤30%, there was the capillary regime of spreading. The drop spread out as a uniform circle in the whole concentration range investigated [54,55]. The area, $S(t)$, covered by solution during the spreading increased in time as $t^{0.2}$. With increasing RH (an unstable region) the spreading process accelerated and the fingering instabilities developed. At the c>CMC, surfactant adsorption at the solid–liquid interface creates a hydrophobic barrier, which increases with surfactant concentration. As a result, the lateral extension of fingers was limited. The total area $S(t)$ covered with solution grows linearly with time, when RH is less than 60%, but at the RH >85% the area increases faster.

The authors [54,55] assumed that surfactant molecules mobility on the substrate induces the instability along the drop edge. However, the adsorbed water film is too thin to provide the motion of surfactant along the substrate. That means the mobility of surfactant controlled by the precursor wetting film ahead of the fingers that goes from the drop under the high humidity. Although the film was not observed directly, indirect evidence of the existing of this film was provided. Dashed lines of non-wettable ink stopped the unbounded spreading of precursor wetting film. As a result the film was thickened in a gap between the drop and the lines. The fingering spreading developed only on that side (Fig. 13).

Subsequent experiments [43] were performed to study the role of precursor wetting film thickness in amplification of the fingering spreading. Thin films of solution of ethylene glycol in methanol were pre-deposited on cleaned silicon wafers. The following surfactant was chosen: $C_{12}E_{10}$ at the fixed CMC (0.02 mol/l) concentration. The humidity was kept around 60%. The thickness of the pre-deposited films were varied from 30 to 250 nm. Under those conditions the advancing line of the surfactant precursor on the pre-deposited film was clearly visible. It allowed revealing that instabilities appear behind the contact line of the solvent film. When the thickness of pre-deposited film was increased, the branching of fingers and the thickness of their tips decreased. The spreading dynamic namely: the finger radius R_f from the centre of drop to their tips and the length of surfactant leading film R_0 were found to scale as $t^{1/2}$, but the radius of the drop, R_c, developed in time as t^{α}, where α was found in the range from 0.3 to 0.45 with increasing the thickness of pre-deposited film.

In [57] the influence of surfactant concentration at the fixed thickness of solvent pre-deposited film on finger formation was studied. At the concentration below the CMC the thick and wide in base fingers were observed. The profile of spreading drop was smooth and no boundary between drop and fingers was observed. For the concentration near the CMC fingers became more straight. At the larger concentration fingers disappeared and a hollow part appeared at the tip of fingers.

In [58,59] the authors investigated the unstable spreading of aqueous solutions of sparingly and highly soluble anionic surfactants in a wide range of surfactant concentration through water films ranging from 25 μm to 100 μm in thickness.

In the case of a sparingly soluble surfactant [58] a 6 μl drop of AOT solution was deposited on the water layer. It was found that the spreading has a stable or a fingering behaviour. At the surfactant concentrations lower than 0.4·CMC, the spreading process was stable for the whole range of thickness investigated and no fingers were observed. During the uniform spreading, the profile of the drop had a disk-like part in the centre with a thickened rim at the advancing edge. For the concentrations in the vicinity of CMC up to 2·CMC the spreading edge of AOT drops was uniform for the several seconds (from 3 to 10 s) that defined by the concentration and the film thickness, then round-tipped and straight fingers appeared behind the thickened rim. The fingers became wider when the concentration decreased and the thickness of water layer increased. The typical spreading rate was found about 0.5 cm/c, and it increased with the water film thickening due to a decreasing of viscous friction. On 25 μm and 50 μm thick films at the concentration 4·CMC, the spreading was stable and uniform with a distinct surfactant covered disk of liquid in the centre of the drop. The latter agrees with the results of Troian et al. [50]. However, on the 100 μm thick film, the fingering spreading behaviour occurred again. Using dimensionless analysis (Peclet numbers) it was shown that Marangoni forces exceed substantially all other forces. The latter showed the dominate role of Marangoni forces in the fingering spreading.

In [59] the role of the surfactant solubility on the fingering instability was considered. In this case, aqueous solutions of a soluble

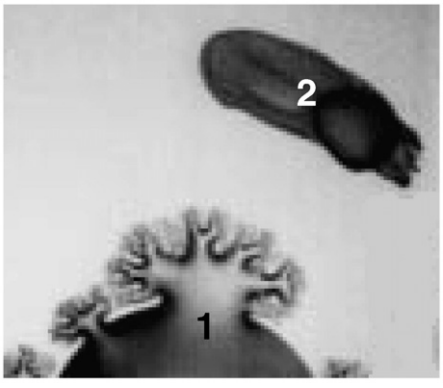

Fig. 13. The faster spreading of $C_{12}E_4$-di-ethylenglycol drop (1) on the side of the non-wettable ink line (2) [54].

surfactant (SDS) were used. Their spreading behaviour shows many similarities with some notable differences to the AOT solution [58]. The spreading rates were of the same order of magnitude for SDS as for AOT. However, in the case of SDS the rate did not vary with the water film thickness. Authors related this fact to fast surfactant desorption and relatively significant influence of gravity force for the high film thickness. The fingers occurred at the SDS concentration of 0.4·CMC, that was two times lower than in the AOT case (0.8·CMC), and almost ten times earlier. The shape of fingers was more pronounced and branched in the result of SDS drop deposition. At the CMC and the high film thickness, the fingering was observed for both surfactants.

Nikolov et al. [60] reported the fingering instabilities during the spreading of drop of aqueous trisiloxane solution (Silwet L-77) on a hydrophobic plate. Their experiments were slightly different from the above reviewed experiments. A distilled water drop was placed on a hydrophobic bottom of polystyrene Petri dish. The water–air interface was covered with hollow glass beads for visualization of the time evolution of the advanced front of drops. A 5 μl droplet of a 0.2 wt.% aqueous trisiloxane solution was placed on the top of the water drop. The drop started to spread immediately at a high rate. In one second at the advanced front fingers were generated and become more pronounced in the course of spreading.

Stoebe et al. [52] observed the small fingers appeared at the edges of droplets of aqueous trisiloxane solutions spreading on the surfaces of various surface energies. The length of fingers was found to be less than 10% of the dynamic droplet radius, that served as a reason to ignore the fingering in the analysis of their experiment.

Poulard et al. [61] addressed the problem of nematic liquid crystals 5CB (cyanobiphenyl) spreading over hydrophilic silicon wafers. The complex interfacial instability in a vicinity of the moving contact line of liquid crystal drops was detected. This instability included two different types of instabilities. The appearance, development and disappearance of the instabilities was modulated by changing the RH of the environment. It was suggested that the small instabilities are the result of the combined effect of elasticity, anchoring defects, and flow, while the secondary instabilities are driven by the flow.

Daniels et al. [62,63] examined spreading dynamics of surfactant Triton X-305 and PDMS drops on a viscoelastic gel agar, which was varied from liquid-like to solid-like state by changing the concentration of agar. The spreading behaviour in this system differed from the typical surfactant spreading on solid substrates and can be described as "an arm-like". An increase of the length of arms, $R(t)$, was described by the power law $R(t) \propto t^{3/4}$. When a droplet was deposited on the gel surface with shear modulus less than 30 Pa, the drop broke into distinct crack-like spreading arms in a starburst formation. On the substrate with shear modulus around 30 Pa, the drop spread uniformly initially, but after a sufficiently long time the droplet demonstrated the wispy morphology. Above 30 Pa, the drops had circular forms as on a pre-wetted solid substrate. It was found that the onset of instabilities and the number of arms (fingers) depend on the ratio of the surface tension gradient to the gel strength.

Troian et al. [46] theoretically investigated the mechanism responsible for the instability during the spreading of surfactant laden drop. Their physical model represents a hemispherical liquid drop covered with insoluble surfactant spreading on a thin layer of the same liquid.

Considerable efforts were invested in the investigation of instabilities in the course of spreading, and the progress was achieved in the understanding of the nature of instabilities.

7. Spreading of surfactant solutions over porous substrates

Spreading and penetration of liquids over/into porous media is a fundamental process with a numerous applications in printing, painting, adhesives, oil recovery, imbibition into soils, health care, and home care products [7,64–68]. In ink-jet printing, the resolution is directly associated to the degree of liquid extension and spreading on the printing medium after deposition [67]. The spreading of a drop on a thin permeable medium proceeds as follows: (a) spreading on the medium surface and (b) penetration into the underlying medium. Knowledge of the spreading rate and the area covered is critical as a drop-to drop contact would results in unwanted and detrimental effects in printing. From other hand, fast penetration of the liquid would limit the time the drop spent on the surface, thereby decreasing coalescence of drops. However, penetration of liquid into porous medium is usually slow due to poor wettability by the liquid of the porous medium. Surfactants from this point of view may play a crucial role.

Surfactants role in oil recovery processes is especially important. It is highly desirable to extract oil trapped in the pores of rocks. The injection of surfactants reduces the interfacial tension between the oil and water phases, allowing the extracting of trapped oil in small pores [68]. The importance of this knowledge leads to on-going research on the wetting kinetics of porous media influenced by surfactants.

Recent publications revealed a growing interest in exploring the simultaneous spreading and imbibition processes of aqueous surfactant solutions. However, these studies have so far mostly been restricted to pure liquids simultaneously spreading and imbibiting into the porous substrate [69–80]. Clarke et al. [81] developed a theoretical model for simultaneous spreading and imbibition by incorporating the molecular-kinetic theory of spreading [71] coupled with a modified Lucas–Washburn equation.

Starov et al. developed a theoretical model [70,82] for the complete wetting case for a drop spreading over a pre-wetted or a dry porous layer. The lubrication theory approximation was used, neglecting gravity influence, so that only capillary forces were taken into account in the model. They developed a system of two differential equations to describe the evolution of the radius of both the drop base, $L(t)$, and wetted region, $l(t)$, inside the porous layer. The latter allowed them to deduce an equation describing the dynamic contact angle. The authors performed experiments in order to test the theoretical model. Silicon oils were the liquid used and nitrocellulose membranes with different pore size were used as porous layers. By comparing the theoretical model and experimental data on appropriate dimensionless scales, a universal behaviour was observed where experimental data was in good agreement with theoretical prediction.

Zhdanov et al. [83] incorporated the previous theoretical model to simulate spreading of surfactant solutions over porous layers. They produced experimental data for the spreading of different concentrations of aqueous SDS solutions over nitrocellulose membranes of different pore sizes, varying drop volume and properties of porous layers. The dynamic contact angle, radius of the spreading droplet, and the wetted perimeter were monitored for the spreading/penetration process. The entire process was divided into 3 stages (Fig. 14). During the first stage, the drop base spreads until it reaches the maximum position whilst contact angle decreases rapidly. The drop base then remains constant during the second stage as the contact angle decreases linearly with time. And finally, the third stage where the drop base shrinks while the contact angle remains constant until the drop completely disappears. During all three stages, the wetted region continued to expand until the final equilibrium value. It was observed that the total duration of spreading, the maximum radius of the drop base, and final radius of the wetted region considerably depend on the drop volume, SDS concentration, averaged pore size and porosity of the membranes used. It is showed that it is more convenient to analyse the experimental data using the same dimensionless values as in the case of spreading of pure liquids over dry porous substrates. The overall spreading time decreases with increasing SDS concentration. Spreading of drops of different volumes (over an identical porous membrane) and the contact angle showed a universal behaviour (Fig. 14) using dimensionless plots. Zhdanov et al. [83] deduced an

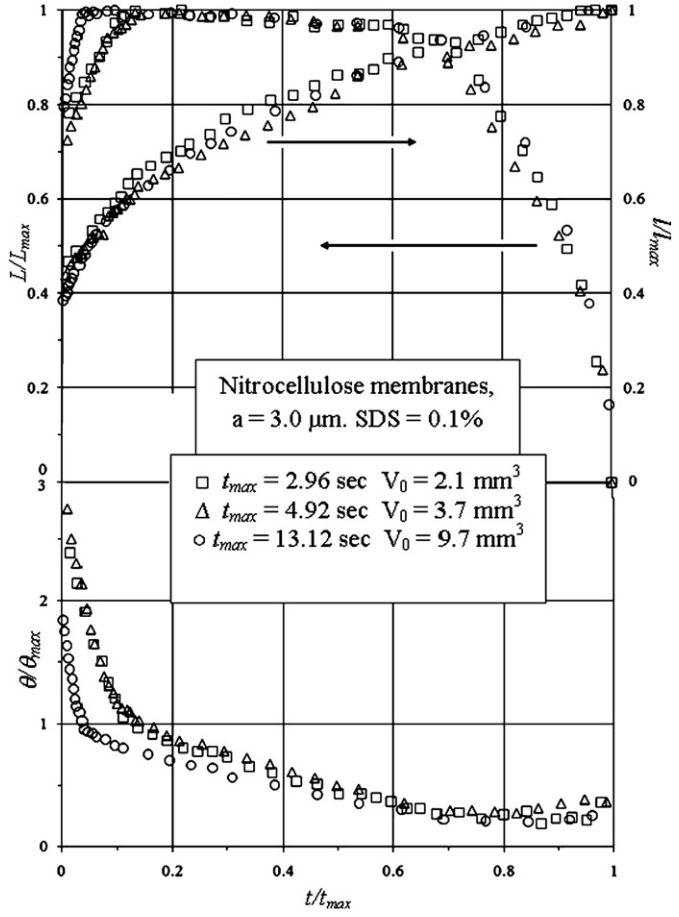

Fig. 14. Spreading of droplets of 0.1% SDS solution over Nitrocellulose membrane, average pore size is 3.0 μm; L/L_{max} is dimensionless radius of the drop base, l/l_{max} is radius of the wetted area, θ/θ_m is dynamic contact angle, t/t_{max} dimensionless time. From [83].

equation that predicts the linear dependency of the contact angle during the second stage of spreading/imbibition process. The contact angle hysteresis (difference between static advancing and static receding contact angles) was plotted extracted to show that this difference becomes smaller with increasing SDS concentration. Independent experiments were performed to conclude the constancy of the contact angle during the third stage. It was concluded that the constancy of the contact angle during the final stage is determined by the hydrodynamic flow only.

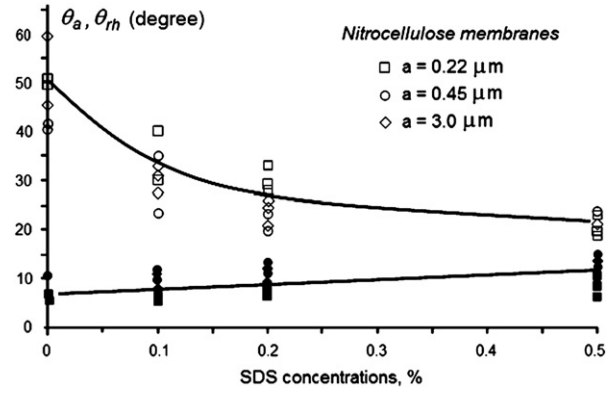

Fig. 15. Porous nitrocellulose substrates. Apparent contact angle hysteresis variation with SDS concentration, Nitrocellulose membranes of different average pore sizes. Open symbols correspond to the advancing contact angle θ_a. The same filled symbols correspond to the hydrodynamic receding contact angle θ_{rh}. From [83].

Using experimental data on drop spreading of aqueous SDS solutions over dry porous substrates the values of advancing, θ_a, and hydrodynamic receding, θ_{rh}, contact angles were extracted as a function of SDS concentration ([83], see an example in Fig. 15). The term "hydrodynamic receding contact angle" and the symbol θ_{rh} was used to distinguish it from the static receding contact angle. The advancing contact angle was defined at the end of the first stage when the drop stopped to spread (the radius of the drop base reached its maximum value). The hydrodynamic receding contact angle θ_{rh} was defined at the moment when the drop base started to shrink. In Fig. 15 experimental data on the apparent contact angle hysteresis are summarized. This figure shows that the advancing contact angle θ_a decreases with SDS concentration; the hydrodynamic receding contact angle θ_{rh} on the contrary slightly increases with SDS concentration. The difference between advancing and receding contact angles becomes smaller with increasing SDS concentration; the dimensionless time interval when the drop base does not move also decreases with the increase of the SDS concentration.

It is necessary to note that the behaviour of drops of aqueous SDS solutions during the third stage of spreading (partial wetting) is remarkably similar to the behaviour during the second stage of spreading in the case of complete wetting section [70,82]. Static advancing and static receding contact angles on smooth non-porous nitrocellulose substrate for different SDS concentrations were also measured to compare with those on porous substrate [83]. The static advancing contact angle of pure water on non-porous nitrocellulose substrate was found equal approximately to 70°. The static advancing contact angle decreases with the increase of SDS concentration (Fig. 16). This trend continues until the CMC is reached. At concentrations above the CMC advancing contact angle remains constant and approximately equals to 35°. Non-zero value of the static receding contact angle was found only in the case of pure water droplets. In all other cases (even at the smallest SDS concentrations used 0.025%) the static receding contact angle was found equal to zero in the all concentration range used: from 0.025% (ten times smaller than CMC) to 1% (five times higher than CMC). A comparison between Figs. 15 and 16 shows that

- The advancing contact angle dependence for porous nitrocellulose substrates on SDS concentration is significantly different from the static advancing contact angle dependence for non-porous nitrocellulose substrates. The latter means that in the case of porous substrates the influence of both the hydrodynamic flow caused by

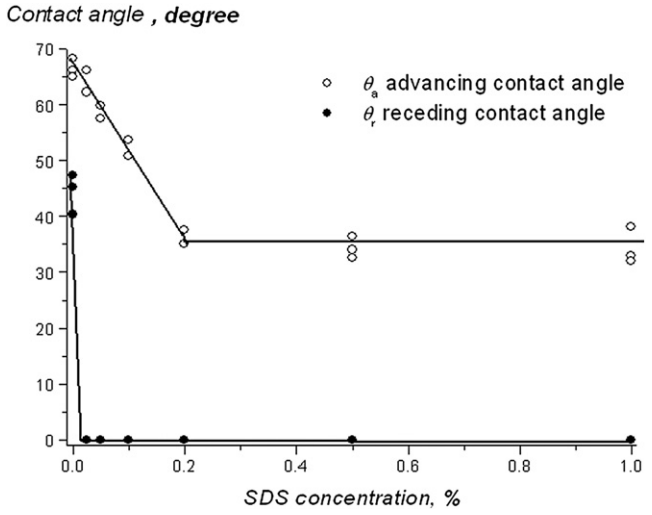

Fig. 16. Non-porous nitrocellulose substrate. Advancing and receding contact angles variation with SDS concentration; open symbols correspond to the static advancing contact angle θ_a; filled symbols correspond to the static receding contact angle θ_r. From [83].

imbibition into the porous substrate and adsorption of surfactants inside pores significantly change the advancing contact angle;
- The hydrodynamic receding contact angle in the case of porous substrates has nothing to do with the hysteresis of the contact angle and determined complete by the hydrodynamic flow in the way similar to the complete wetting case.

Daniel et al. [84] developed a model to predict the simultaneous spreading and penetration of surfactant solutions based on energy considerations of the system. A comparison with [70] showed the energy based model is functionally equivalent. The derived energy based model was tested against experimental data on spreading of commercial surfactants over a variety of papers relevant to thermal ink-jet printing.

It is necessary to emphasise that in spite of enormous industrial importance the kinetics of spreading/imbibition of surfactant solutions into porous media is still far less investigated than it deserves.

8. Superspreading

Silicone surfactants (particularly trisiloxanes) have been subjected to substantial interest since early 90 s. Trisiloxane surfactants are commonly denoted as M(D'E_n)M, where M stands for the trimethylsiloxy group, $(CH_3)_3$–$SiO_{1/2}$–, the term D' stands for the –$O_{1/2}$Si(CH_3)(R)$O_{1/2}$–, where R is a polyoxyethylene group attached to the silicon, and E_n stands for polyoxyethylene, –$(CH_2$–$CH_2O)_nR$–. For simplicity, trisiloxane with n polyoxyethylene group will be referred to as T_n. Trisiloxanes were found to possess an unusual ability to induce highly efficient wetting properties of hydrophobic surfaces under appropriate conditions and, hence, the term "superspreading" became associated with trisiloxanes.

Unusual wetting properties of trisiloxanes were discussed in [85,86]. The overall spread area achievable by an aqueous droplet containing trisiloxane surfactant can be as much as 50 times greater than of pure water, and 25 times more effective than conventional surfactants [60]. Commercially available trisiloxane surfactant, Silwet® L-77™ (L-77), are polydispersed with an average of 7.5 ethoxylate groups, has been widely used since discovered in the late eighties [87]. Fig. 17 illustrates this point by comparing the relative spreading properties of water with 0.25% Triton X-100 (polyoxythylene (10)-octylphenyl ether) and with aqueous solution of 0.1% S-77 surfactant on a velvetleaf (Abutilion theophrasti). Water alone on velvetleaf makes a contact angle bigger than 90°, aqueous Triton X-100 solution gives a larger spreading area. However, L-77 provides a significant increase in the spreading area and decrease in contact angle making it an effective wetting agent. This was supported by [85,88] concluding that T_8 has one of the best wetting properties.

The superspreading phenomenon attracted much attention both from the theoretical point of view and because of the practical use of the phenomenon. However, there is no general agreement about the mechanism of the effect and on the necessary conditions for its realization.

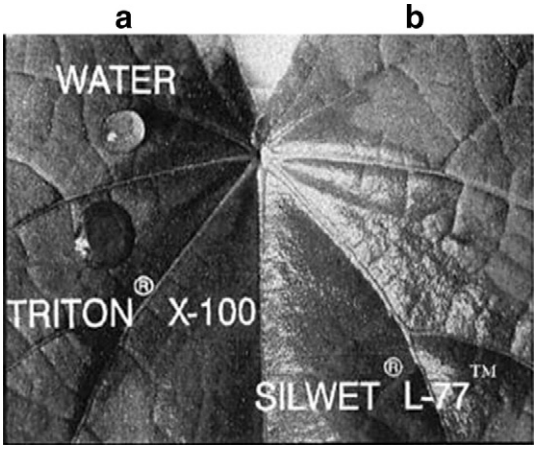

Fig. 17. Photograph [60] depicting the spreading of (a) a water drop and a drop of 0.25% Triton X-100 solution; (b) 0.1% L-77 solution on a velvetleaf surface.

The wetting behaviour of the trisiloxane surfactant solution is usually attributed to its ability to adsorb at the liquid–vapour and hydrophobic solid–liquid interfaces at the moving TPC line and to reduce considerably the tensions of these interfaces, creating a positive spreading coefficient. The rapid spreading can be due to maintaining a positive spreading coefficient at the perimeter as the drop spreads. However, the liquid–vapour and solid–liquid interfaces at the perimeter are depleted of surfactant by interfacial expansion as the drop spreads. The spreading coefficient can remain positive if the rate of surfactant adsorption onto the solid and fluid surfaces from the spreading aqueous film at the perimeter exceeds the diluting effect due to the area expansion. This becomes even more difficult if we take into account that the reservoir of surfactant in the droplet is continually depleted by adsorption to the expanding interfaces. If the adsorption cannot keep pace with the area expansion at the perimeter, and the surface concentrations become reduced at the contact line, a negative spreading coefficient can develop, which retards the drop movement. Unfortunately, the latter explanation can be equally applied to any aqueous surfactant solution and unfortunately is not specific for trisiloxanes.

Aqueous drops with dissolved trisiloxane at sufficiently high bulk concentration, usually several times their critical aggregation concentration (CAC) [87,89–91], when placed on hydrophobic surfaces, rapidly spread out and completely wet the substrate with no measurable final contact angle. It was reported in [91,92] that a critical wetting concentration (CWC) exists for trisiloxane solutions at spreading over solid and liquid substrates. Ruckenstein [93] assumed that formation of surfactant multilayer adsorption is a possible reason for fast spreading to occur. In [94] the argument on the occurrence of a transition at the CWC from partial wetting to complete spreading were presented. Three regimes of the spreading dynamics were observed in [94]: early stages where wetting diameter is proportional to t^n with n in the range 0.12–0.22; during the second stage the exponent increases to 0.38–0.58; during the last stage of spreading the surface roughness and local tension gradients lead to asymmetric drop shape and formation of fingers and dendrites.

Marangoni mechanism can contribute to the rapid spreading: the surface concentrations at the drop apex remains higher as compared to the perimeter so that the drop can be pulled out by the higher tension at the perimeter than at the drop apex. To maintain a high apex concentration, surfactant adsorption must exceed the rate of interfacial dilation at the apex due to the outward flow. Nikolov et al. [60] and Chengara et al. [95] investigated the influence of Marangoni mechanism on superspreading. They provided evidence that surface tension gradient is an important driving force in superspreading. They found maxima in spreading rates versus concentrations.

Ananthapadmanabhan et al. [88] postulated that the rapid spreading is a result of a peculiar character of the trisiloxane moiety, its wide hydrophobic group. However, it was later shown that molecular geometry probably is not a critical parameter [96,97].

Solution turbidity, i.e. the presence of disperse phase, was found to be an important parameter. This follows from experiments with the aqueous solutions of trisiloxane surfactant, T_8, performed by Zhu et al. [87]. These authors suggested that superspreading occurs only when dispersed particles (vesicles) are present. They also showed that the rate of droplet spreading over Parafilm, increases with concentration and reaches a maximum. The authors also noticed that sonicated solutions spread faster. Addition of formamide reduces the amount of dispersed phase and results in a decrease of the rate of spreading and the spreading area. Stoebe et al. [97] observed that aqueous trisiloxane surfactant solutions effectively wet substrates with slightly higher surface energy than those previously investigated.

Formation of vesicle type aggregates is a requirement for trisiloxane induced superspreading [85,97]. It was concluded [96,98]

that in the range of 0.01–0.25wt.%, trisiloxane solutions contain vesicles. These vesicles and/or other aggregates disintegrate to efficiently transfer surfactant molecules to the contact surfaces and enhance spreading [97].

However, Nikolov et al.[60] showed that although the aggregates are present in the solution, it does not play so important part in initiating the Marangoni effect, which is a cause of superspreading according to their opinion.

A number of hypothesis for the explanation of the superspreading phenomenon were put forward including configuration of the trisiloxane molecules at the interfaces [88,96,97], or the formation of a precursor film on a solid surface [97]. Zhu et al. [87] noted the influence of the water-vapour pressure in the surrounding atmosphere on the superspreading. Superspreading of T_8 solutions was observed only in the presence of saturated or supersaturated water vapour. This has given rise to the suggestion that fast spreading may be caused by surface flow of a thin precursor film formed from the vapour phase. Churaev et al. [99] found climbing of thick films (around 4 μm) of trisiloxane surfactant solutions over hydrophobic surfaces against the gravity action. They suggested that the superspreading is caused by formation of those extremely thick wetting films of the solution. Existence and stability of such micron thick films may be explained by the action of repulsive forces between dispersed particles (vesicles), that is, extremely long ranged surface forces.

Acknowledgements

K. S. Lee, N. Ivanova, V.M. Starov and N. Hilal would like to acknowledge the support from the Engineering and Physical Sciences Research Council, UK (Grant EP/D077869/1). V. Dutschk is indebted to Dr. B. Breitzke and Dr. M. Stolz (both from Sasol Germany) for the many valuable discussions as well as to Sasol Germany (Marl) for the financial support.

References

[1] Cox RG. J Fluid Mech 1986;168:169.
[2] Voinov OV. Fluid Dyn 1976;11:714.
[3] Blake TD, Haynes JM. J Colloid Interface Sci 1969;30:421.
[4] Chibowski E. Adv Colloid Interface 2007;133:51.
[5] Exerowa D, Krugliakov P. In foam and foam films: theory, experiment, application. Studies in interface Science, vol. 5. New York: Elsevier; 1998.
[6] Churaev N, Zorin Z. Adv Colloid Interface 1992;40:109.
[7] Starov V, Velarde M, Radke C. In dynamics of wetting and spreading. Surfactant Sciences Series, vol. 138. Taylor & Frances; 2007.
[8] Keurentjes JTF, Cohen Stuart MA, Brinkman D, Schroen CGPH, van Riet K. Colloid Surf 1990;51:89.
[9] Scales PJ, Grieser F, Furlong DN, Healy TW. Colloid Surf, A Physicochem Eng Asp 1986;21:55.
[10] von Bahr M, Tiberg F, Yaminsky V. Colloid Surf, A Physicochem Eng Asp 2001;193:85.
[11] Dutschk V, Sabbatovskiy KG, Stolz M, Grundke K, Rudoy VM. J Colloid Interfaces Sci 2003;267:456.
[12] Starov VM, Kosvintsev SR, Velarde MG. J Colloid Interface Sci 2000;227:185.
[13] Churaev N, Zorin Z. Colloids Surf, A Physicochem Eng Asp 1995;100:131.
[14] Zolotarev PP, Starov VM, Churaev NV. Colloid J R Acad Sci, English Translation) 1976;38:895.
[15] Churaev NV, Martynov GA, Starov VM, Zorin ZM. Colloid Polym Sci 1981;259:747.
[16] Dutschk V, Breitzke B. Tenside Surfactants Deterg 2005;42:82.
[17] Dutschk V, Breitzke B, Grundke K. Tenside Surfactants Deterg 2003;40:250.
[18] Eriksson J, Tiberg F, Zhmud B. Langmuir 2001;17:7274.
[19] Frank B, Garoff S. Colloids Surf, A Physicochem Eng Asp 1996;116:31.
[20] Chan KY, Borhan A. J Colloid Interface Sci 2005;287:233.
[21] Washburn EW. Phys Rev 1921;17:273.
[22] Zhmud BV, Tiberg F, Halstensson K. J Colloid Interface Sci 2000;228:263.
[23] Laurent T, Thierry L, Liviu N. J Appl Phys 2007;101:044907.
[24] Sammarco TS, Burns MA. AICHE J 1999;45:350.
[25] Starov VM. J Colloid Interface Sci 2004;270:180.
[26] Starov VM. Adv Colloid Interface Sci 2004;111:3.
[27] Tiberg F, Zhmud B, Hallstensson K, von Bahr M. Phys Chem Chem Phys 2000;2:5189.
[28] Bain CD. Phys Chem Chem Phys 2005;7:3048.
[29] Starov VM, Zhdanov SA, Velarde MG. J Colloid Interface Sci 2004;273:589.
[30] Hodgson KT, Berg JC. J Colloid Interface Sci 1988;121:22.
[31] Schwartz LW, Weidner DE, Eley RR. Proc ACS Div Polym Mater Sci Eng 1995;73:490.
[32] Patzer J, Fuchs J, Hoffer EP. Proc SPIE Int Soc Opt Eng 1995;167:2413.
[33] Le HP. J Imaging Sci Techn 1998;42:49.
[34] Shapiro DL. In surfactant replacement therapy; 1989. AR Liss, New York.
[35] Tsai W, Liu L. Colloids Surf, A Physicochem Eng Asp 2004;234:51.
[36] Bierwagen GP. Prog Org Coat 1991;19:59.
[37] Gundabala VR, Routh AF. J Colloid Interface Sci 2006;303:306.
[38] Chang InSoung, Kim JaeHyung. J Clean Prod 2001;9:227.
[39] Afsar-Siddiqui AB, Luckham PF, Matar OK. Adv Colloid Interface 2003;106:183.
[40] Lee KS, Starov VM. J Colloid Interface Sci 2007;314:631.
[41] Starov VM, de Ryck A, Velarde MG. J Colloid Interface Sci 1997;190:104.
[42] Marmur A, Lelah MD. Chem Eng Commun 1981;13:133.
[43] Cachile M, Schneemilch M, Hamraoui A, Cazabat AM. Adv Colloid Interface 2002;96:59.
[44] Borgas MS, Grotberg JB. J Fluid Mech 1988;193:151.
[45] Gaver PD, Grotberg JB. J Fluid Mech 1990;213:127.
[46] Troian SM, Herbolzheimer E, Safran SA. Phys Rev Lett 1990;65:333.
[47] Jensen OE, Grotberg JB. J Fluid Mech 1992;240:259.
[48] Jensen OE. J Fluid Mech 1995;240:349.
[49] Princen HM, Cazabat AM, Cohen Stuart MA, Heslot F, Nicolet S. J Colloid Interface Sci 1988;126:84.
[50] Troian SM, Wu XL, Safran SA. Phys Rev Lett 1989;62:1496.
[51] Frank B, Garoff S. Langmuir 1995;11:87.
[52] Stoebe T, Lin Z, Hill RM, Ward MD, Davis HT. Langmuir 1996;12:337.
[53] Stoebe T, Lin Z, Hill RM, Ward MD, Davis HT. Langmuir 1997;13:7282.
[54] Cachile M, Cazabat AM. Langmuir 1999;15:1515.
[55] Cachile M, Cazabat AM, Bardon S, Valignat MP, Vandenbrouck F. Colloids Surf 1999;159:47.
[56] Cachile A, Albisu G, Calvo A, Cazabat AM. Physica A 2003;329:7.
[57] Hamraoui A, Cachile M, Poulard C, Cazabat AM. Colloids Surf, A Physicochem Eng Asp 2004;250:215.
[58] Afsar-Siddiqui AB, Luckham PF, Matar OK. Langmuir 2003;19:692.
[59] Afsar-Siddiqui AB, Luckham PF, Matar OK. Langmuir 2003;19:703.
[60] Nikolov AD, Wasan DT, Chengara A, Koczo K, Policellob GA, Kolossvary I. Adv Colloid Interface 2002;96:325.
[61] Poulard C, Cazabat AM. Langmuir 2005;21:6270.
[62] Daniels KE, Mukhopadhyay S, Behringer RP. Chaos 2005;15:041107.
[63] Daniels KE, Mukhopadhyay S, Houseworth PJ, Behringer RP. Phys Rev Lett 2007 arXiv:cond-mat/0606296v2 [cond-mat.soft].
[64] Kumar SM, Deshpande AP. Colloid Surf, A Physicochem Eng Asp 2006;277:157.
[65] Maiti RN, Khanna R, Sen PK, Nigam KDP. Chem Eng Sci 2004;59:2817.
[66] Maiti RN, Arora R, Khanna R, Nigam KDP. Chem Eng Sci 2005;60:6235.
[67] Holman RK, Cima MJ, Uhland SA, Sachs E. J Colloid Interface Sci 2002;249:432.
[68] Lake LW. Enhanced Oil Recovery. Englewood Cliffs, NJ: Prentice-Hall; 1996.
[69] Starov VM, Zhdanov SA, Velarde MG. J Colloid Interface Sci 2004;273:589.
[70] Starov VM, Kosvintsev SR, Sobolev VD, Velarde MG, Zhdanov SA. J Colloid Interface Sci 2002;252:397.
[71] Blake TD, Clarke A, DeConnick J, de Ruijter MJ. Langmuir 1997;13:2164.
[72] Davis SH, Hockings LM. Phys Fluids 1999;11:48.
[73] Aradian A, Raphael E, de Gennes PG. Eur Phys J E 2000;2:367.
[74] Bacri L, Brochard-Wyart F. Eur Phys J E 2000;3:87.
[75] Alleborn N, Raszillier H. J Colloid Interface Sci 2004;280:449.
[76] Alleborn N, Raszillier H. Chem Eng Sci 2004;59:2071.
[77] Modaressi H, Garnier G. Langmuir 2002;18:642.
[78] Heilmann J, Lindqvist U. J Imaging Sci Technol 2002;44:491.
[79] Heilmann J, Lindqvist U. J Imaging Sci Technol 2002;44:495.
[80] Denesuk M, Zelinski BJJ, Kreidi NJ, Uhlmann DR. J Colloid Interface Sci 1994;168:142.
[81] Clarke A, Blake TD, Carruthers K, Woodward A. Langmuir 2002;18:2980.
[82] Starov VM, Zhdanov SA, Kosvintsev SR, Sobolev VD, Velarde MG. Adv Colloid Interface 2003;104:123.
[83] Zhdanov SA, Starov VM, Sobolev VD, Velarde MG. J Colloid Interface Sci 2003;264:481.
[84] Daniel RC, Berg JC. Adv Colloid Interface 2006;439:123.
[85] Hill RM. Curr Opin Colloid Interface 1998;3:247.
[86] Hill RM. Curr Opin Colloid Interface 2002;7:255.
[87] Zhu S, Miller WG, Scriven LE, Davis HT. Colloids Surf, A Physiochem Eng Asp 1994;90:63.
[88] Ananthapadmanabhan KP, Goddard ED, Chandar P. Colloids Surf 1990;44:281.
[89] Lin Z, Hill RM, Davis HT, Ward MD. Langmuir 1994;10:4060.
[90] Lin Z, Stoebe T, Hill RM, Davis HT, Ward MD. Langmuir 1996;12:345.
[91] Svitova T, Hill RM, Smirnova Y, Stuermer A, Yakubov G. Langmuir 1998;14:5023.
[92] Svitova T, Hill RM, Radke CJ. Langmuir 1999;15:7392.
[93] Ruckenstein E. J Colloid Interface Sci 1996;179:136.
[94] Svitova T, Hill RM, Radke CJ. Colloids Surf, A Physiochem Eng Asp 2001;607:183–5.
[95] Chengara A, Nikolov A, Wasan D. Colloids Surf, A Physiochem Eng Asp 2002;206:31.
[96] Hill R, He M, Davis H, Scriven L. Langmuir 1994;10:1724.
[97] Stoebe T, Lin Z, Hill R, Ward D, Davis T. Langmuir 1997;13(26):7270 7276.
[98] He M, Hill R, Lin Z, Scriven L, Davis H. J Phys Chem 1993;97:8820.
[99] Churaev NV, Esipova NE, Hill RM, Sobolev VD, Starov VM, Zorin ZM. Langmuir 2002;17:1338.